Lattice Gauge Theory with Cold Atoms and Quantum Computers

Yannick Meurice

The University of Iowa

yannick-meurice@uiowa.edu

With Alexei Bazavov, Sam Foreman, Erik Gustafson, Yuzhi Liu, Philipp Preiss, Shan-Wen Tsai, Judah Unmuth-Yockey (talk on Thursday), Li-Ping Yang, Johannes Zeiher, and Jin Zhang

Supported by the Department of Energy

ECT, June 11, 2019

Content of the talk

- Quantum computations/simulations for high energy physics?
- Strategy:
  - big goals with enough intermediate steps
  - explore as many paths as possible
  - leave room for serendipity
- Tensor tools: QC friends and competitors (RG)
- Symmetry preserving truncations (YM, arxiv:1903.01918)
- Entanglement entropy and central charge from twin atomic tubes (Phys.Rev. A96)
- Quantum Joule experiments (arXiv:1903.01414, with Jin Zhang and Shan-Wen Tsai)
- Abelian Higgs model with cold atoms (PRL 121, see Judah Unmuth-Yockey's talk)
- Quantum computations (digital): IBM, IonQ, Rigetti, ...
- Benchmark for real time scattering (arXiv:1901.05944, PRD 99 094503 with Erik Gustafson and Judah Unmuth-Yockey)
- Conclusions

Quantum computations/simulations for high energy physics?

Problems where perturbation theory and classical sampling fail:

- Real-time evolution for QCD
- Jet Physics (crucial for the LHC program)
- Finite density QCD (sign problem)
- Near conformal systems (BSM, needs very large lattices)
- Early cosmology
- Strong gravity

Strategy: many intermediate steps towards big goals

- High expectations for quantum computing (QC): new materials, fast optimization, security, ...
- Risk management: theoretical physics is a multifaceted landscape
- Lattice gauge theory lesson: big goals can be achieved with small steps
- Example of a big goal: ab-initio jet physics
- Examples of small steps: real-time evolution in 1+1 Ising model, 1+1 Abelian Higgs model, Schwinger model, 2+1 $U(1)$ gauge theory ,....
- Many possible paths: quantum simulations (trapped ions, cold atoms,...), quantum computations (IBM, Rigetti,...)
- Small systems are interesting: use Finite Size Scaling (data collapse, Luscher's formula,....)

Jet Physics ab initio: a realistic long term goal?

Pythia, Herwig, and other jet simulation models encapsulate QCD ideas, empirical observations and experimental data. It is crucial for the interpretation of collider physics experiments. Could we recover this understanding from scratch (ab-initio lattice QCD)?

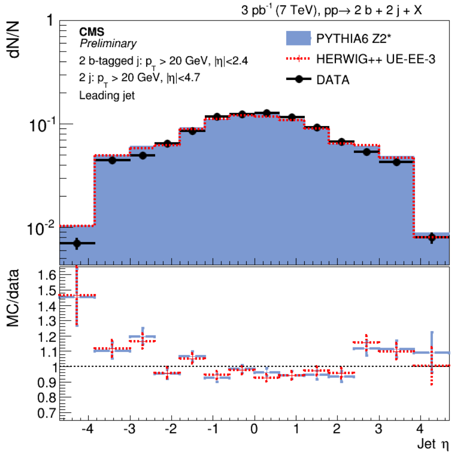

Lessons from lattice gauge theory

We need to start with something simple!

Figure: Mike Creutz's calculator used for a Z_2 gauge theory on a 3^4 lattice (circa 1979).

Following the “Kogut sequence"

An introduction to lattice gauge theory and spin systems*

John B. Kogut

Department of Physics, University of Illinois at Urbana-Champaign, Urbana, Illinois 61801

This article is an interdisciplinary review of lattice gauge theory and spin systems. It discusses the fundamentals, both physics and formalism, of these related subjects. Spin systems are models of magnetism and phase transitions. Lattice gauge theories are cutoff formulations of gauge theories of strongly interacting particles. Statistical mechanics and field theory are closely related subjects, and the connections between them are developed here by using the transfer matrix. Phase diagrams and critical points of continuous transitions are stressed as the keys to understanding the character and continuum limits of lattice theories. Concepts such as duality, kink condensation, and the existence of a local, relativistic field theory at a critical point of a lattice theory are illustrated in a thorough discussion of the two-dimensional Ising model. Theories with exact local (gauge) symmetries are introduced following Wegner's Ising lattice gauge theory. Its gauge-invariant “loop” correlation function is discussed in detail. Three – dimensional Ising gauge theory is studied thoroughly. The renormalization group of the two dimensional planar model is presented as an illustration of a phase transition driven by the condensation of topological excitations. Parallels are drawn to Abelian lattice gauge theory in four dimensions. Non-Abelian gauge theories are introduced and the possibility of quark confinement is discussed. Asymptotic freedom of O(n) Heisenberg spin systems in two dimensions is verified for $n \geq$ and is explained in . simple terms. The direction of present-day research is briefly reviewed.

CONTENTS

I. INTRODUCTION—AN OVERVIEW OF THIS ARTICLE

This article consists of a series of introductory lectures on lattice gauge theory and spin systems. It is intended to explain some of the essentials of these subjects to students interested in the field and research physicists whose expertise lies in other domains. The expert in lattice gauge theory will find little new in the following pages aside from the author's personal perspective and overview. The style of this presentation is informal. The article grew out of a half-semester graduate course on lattice physics presented at the University of Illinois during the fall semester of 1978.

Lattice spin systems are familiar to most physicists because they model solids that are studied in the laboratory. These systems are of considerable interest in these lectures, but we shall also be interested in more abstract questions. In particular, we shall be using space–time lattices as a technical device to define cutoff field theories. The eventual goal of these studies is to construct solutions of cutoff theories so that field theories defined in real continuum Minkowski space–time can be understood. The lattice is mere scaffolding—an intermediate step used to analyze a difficult nonlinear system of an infinite number of degrees of freedom. Different lattice formulations of the same

* Supported in part by the National Science Foundation under grant number NSF PHY77-25279.

III. The Transfer Matrix—Field Theory and Statistical Mechanics 664
A. General remarks 664
B. The path integral and transfer matrix of the simple harmonic oscillator 664
C. The transfer matrix for field theories 666
IV. The Two-Dimensional Ising Model 669
A. Transfer matrix and τ-continuum formulation 669
B. Self-duality of the Ising model 671
C. Strong coupling expansions for the mass gap, weak coupling expansions for the magnetization 672
D. Kink condensation and disorder 676
E. Self-duality of the isotropic Ising model 677
F. Exact solution of the Ising model in two dimensions 678
V. Wegner's Ising Lattice Gauge Theory 681
A. Global symmetries, local symmetries, and the energetics of spontaneous symmetry breaking 681
B. Constructing an Ising model with a local symmetry 682
C. Elitzur's theorem—the impossibility of spontaneously breaking a local symmetry 683
D. Gauge-invariant correlation functions 684
E. Quantum Hamiltonian and phases of the three-dimensional Ising gauge theory 686
VI. Abelian Lattice Gauge Theory 689
A. General formulation 689
B. Gauge-invariant correlation functions, physical interpretations, and phase diagrams 690
C. The quantum Hamiltonian formulation and quark confinement 694
VII. The Planar Heisenberg Model in Two Dimensions 696
A. Introductory comments and motivation 696
B. The physical picture of Kosterlitz and Thouless 697

Figure: Cover page of J. Kogut RMP 51 (1979).

Discretization of problems intractable with classical computing

Quantum computing (QC) requires a complete discretization of QFT

- Discretization of space: lattice gauge theory formulation
- Discretization of field integration: tensor methods for compact fields (as in Wilson lattice gauge theory and nonlinear sigma models, the option followed here)
- QC methods for scattering in ϕ^4 (non-compact) theories are discussed by JLP (Jordan Lee Preskill)
- JLP argue that QC is necessary because of the asymptotic nature of perturbation theory (PT) in λ for ϕ^4 and propose to introduce a field cut (but this makes PT convergent! YM PRL 88 (2002))
- Non compact fields methods ($\lambda\phi^4$) see: Macridin, Spentzouris, Amundson, Harnik, PRA 98 042312 (2018) (fermions+bosons) and Klco and Savage arXiv:1808.10378 and 1904.10440.

Important ideas of the tensor reformulation

- In most lattice simulations, the variables of integration are compact and character expansions (such as Fourier series) can be used to rewrite the partition function and average observables as discrete sums of contracted tensors.
- The “hard" integrals are done exactly and then field integrations provide Kronecker deltas. Example: the $O(2)$ model (I_n : Bessel)

$$e^{\beta \cos(\theta_i - \theta_j)} = \sum_{n_{ij}=-\infty}^{+\infty} e^{in_{ij}(\theta_i - \theta_j)} I_{n_{ij}}(\beta)$$

- This reformulations have been used for RG blocking but they are also suitable for quantum computations/simulations when combined with truncations.
- Important features:
    - Truncations do not break global symmetries
    - Standard boundary conditions can be implemented
    - Matrix Product State ansatzs are exact

From compact to discrete

O(2) model

$$Z = \prod_x \int_{-\pi}^{\pi} d\theta_x \; e^{\beta \sum_{\langle xy\rangle} \cos(\theta_x - \theta_y)} = I_0^V(\beta)\, \mathrm{Tr}_{\{n,m\ldots\}} \prod_x T^{(x)}_{n_x n'_x m_x m'_x}$$

↳ nearest neighbor

$$e^{\beta \cos(\theta_x - \theta_y)} = \sum_{n_{xy}} e^{i n_{xy}(\theta_x - \theta_y)} I_{n_{xy}}(\beta)$$

$$\prod_x \int_{-\pi}^{\pi} d\theta_x \longrightarrow \sum_{\{n\}}$$

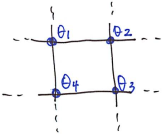

continuous
compact

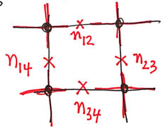

discrete
infinite

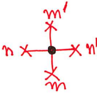

$$: \; T_{nn'mm'} = \sqrt{t_n t_{n'} t_m t_{m'}}\; \delta_{n+m,\, n'+m'}$$

$$t_n = I_n(\beta)/I_0(\beta)$$

Tensor Renormalization Group (TRG)

- TRG: first implementation of Wilson program for lattice models with controllable approximations; no sign problems; truncation methods need to be optimized
- Models we considered: Ising model, $O(2)$, $O(3)$, principal chiral models, gauge models (Ising, $U(1)$ and $SU(2)$))
- Used for quantum simulators, measurements of entanglement entropy, central charge, Polyakov's loop ...
- Our group: PRB 87 064422 (2013), PRD 88 056005 (2013), PRD 89 016008 (2014), PRA90 063603 (2014), PRD 92 076003 (2015), PRE 93 012138 (2016) , PRA 96 023603 (2017), PRD 96 034514 (2017), PRL 121 223201 (2018), PRD 98 094511 (2018)
- Basic references for tensor methods for Lagrangian models: Levin and Nave, PRL 99 120601 (2007), Z.C. Gu et al. PRB 79 085118 (2009), Z. Y. Xie et al., PRB 86 045139 (2012)
- Schwinger model/fermions/CP(N): Yuya Shimizu, Yoshinobu Kuramashi; Ryo Sakai, Shinji Takeda; Hikaru Kawauchi.

TRG blocking: simple and exact!

For each link:

$$\exp(\beta\sigma_1\sigma_2) = \cosh(\beta)(1 + \sqrt{\tanh(\beta)}\sigma_1\sqrt{\tanh(\beta)}\sigma_2) =$$
$$cosh(\beta)\sum_{n_{12}=0,1}(\sqrt{\tanh(\beta)}\sigma_1\sqrt{\tanh(\beta)}\sigma_2)^{n_{12}}.$$

Regroup the four terms involving a given spin σ_i and sum over its two values ± 1. The results can be expressed in terms of a tensor: $T^{(i)}_{xx'yy'}$ which can be visualized as a cross attached to the site *i* with the four legs covering half of the four links attached to *i*. The horizontal indices $x,\ x'$ and vertical indices $y,\ y'$ take the values 0 and 1 as the index n_{12}.

$$T^{(i)}_{xx'yy'} = f_x f_{x'} f_y f_{y'} \delta\left(\mathrm{mod}[x + x' + y + y', 2]\right) \ ,$$

where $f_0 = 1$ and $f_1 = \sqrt{\tanh(\beta)}$. The delta symbol is 1 if $x + x' + y + y'$ is zero modulo 2 and zero otherwise.

TRG blocking (graphically)

Exact form of the partition function: $Z = (\cosh(\beta))^{2V} \mathrm{Tr} \prod_i T^{(i)}_{xx'yy'}$.
Tr mean contractions (sums over 0 and 1) over the links.
Reproduces the closed paths ("worms") of the HT expansion.
TRG blocking separates the degrees of freedom inside the block which are integrated over, from those kept to communicate with the neighboring blocks. Graphically :

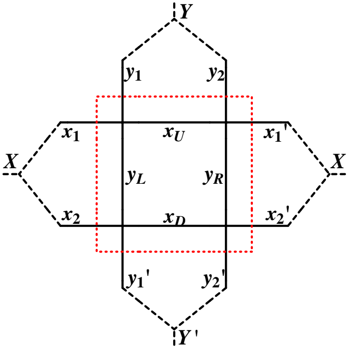

TRG Blocking (formulas)

Blocking defines a new rank-4 tensor $T'_{XX'YY'}$ where each index now takes four values.

$$T'_{X(x_1,x_2)X'(x'_1,x'_2)Y(y_1,y_2)Y'(y'_1,y'_2)} = \sum_{x_U,x_D,x_R,x_L} T_{x_1 x_U y_1 y_L} T_{x_U x'_1 y_2 y_R} T_{x_D x'_2 y_R y'_2} T_{x_2 x_D y_L y'_1} \ ,$$

where $X(x_2, x_2)$ is a notation for the product states e. g. , $X(0,0) = 1,\ X(1,1) = 2,\ X(1,0) = 3,\ X(0,1) = 4$. The partition function can be written exactly as

$$Z = (\cosh(\beta))^{2V} \mathrm{Tr} \prod_{2i} T'^{(2i)}_{XX'YY'} \ ,$$

where $2i$ denotes the sites of the coarser lattice with twice the lattice spacing of the original lattice. Using a truncation in the number of “states" carried by the indices, we can write a fixed point equation.

TRG is a competitor for QC: CPU time $\propto \log(V)$ with no sign problems (both sides will benefit!)

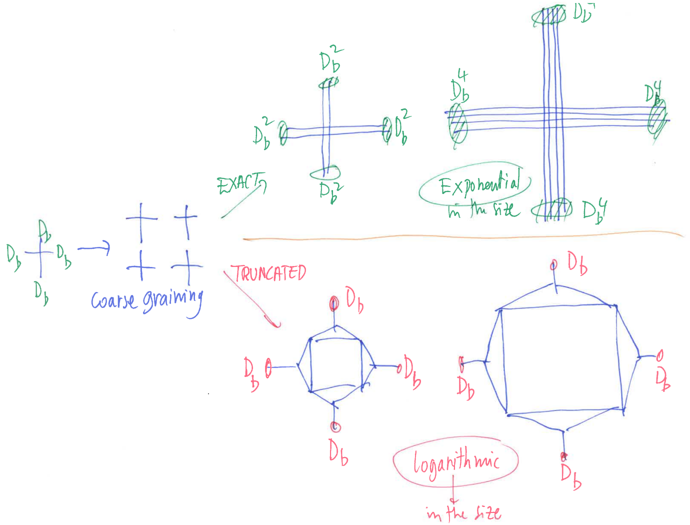

FAQ: Do truncations break global symmetries? No (Y.M. arXiv 1903.01918)

- Truncations of the tensorial sums are necessary, but do they break the symmetries of the model?
- arXiv 1903.01918: non-linear O(2) sigma model and its gauged version (the compact Abelian Higgs model), on a D-dimensional cubic lattice: truncations are compatible with symmetry identities.
- This selection rule is due to the quantum number selection rules at the sites and is independent of the particular values taken by the tensors (e. g. 0, discrete form of a vector calculus theorem).
- Extends to global $O(3)$ symmetries (you need to keep all the m's for a given ℓ, similar to $\langle g|\ell m m'\rangle \propto D^j_{mm'}(g)$ by Burello and Zohar, PRD 91) and pure gauge $U(1)$.
- The universal properties of these models can be reproduced with highly simplified formulations desirable for implementations with quantum computers or for quantum simulations experiments.

Basic identity for symmetries in lattice models

- Generic lattice model with action $S[\Phi]$
- Φ denotes a field configuration of fields ϕ_ℓ attached to locations ℓ which can be sites, links, plaquettes or higher dimensional objects
- Partition function: $Z = \int \mathcal{D}\Phi \mathrm{e}^{-S[\Phi]}$,
- Expectation values: $\langle f(\Phi) \rangle = \int \mathcal{D}\Phi f(\Phi) \mathrm{e}^{-S[\Phi]}/Z$
- Symmetry: field transformations $\phi_\ell \to \phi'_\ell = \phi_\ell - \delta\phi_\ell[\Phi]$ such that:

$$\mathcal{D}\Phi' = \mathcal{D}\Phi \text{ and } S[\Phi'] = S[\Phi].$$

- This implies: $\langle f(\Phi) \rangle = \langle f(\Phi + \delta\Phi) \rangle.$

The O(2) model (Ising model with spin on a circle)

The integration measure $\int \mathcal{D}\Phi = \prod_x \int_{-\pi}^{\pi} \frac{d\varphi_x}{2\pi}$

and the action $S[\Phi] = -\beta \sum_{x,i} \cos(\varphi_{x+\hat{i}} - \varphi_x)$are both invariant under the global shift

$$\varphi'_x = \varphi_x + \alpha$$

This implies that for a function f of N variables

$$\langle f(\varphi_{x_1}, \ldots, \varphi_{x_N}) \rangle = \langle f(\varphi_{x_1} + \alpha, \ldots, \varphi_{x_N} + \alpha) \rangle$$

Since f is 2π-periodic and can be expressed in terms Fourier modes

$$\left\langle \mathrm{e}^{(i(n_1\varphi_{x_1} + \ldots n_N\varphi_{x_N}))} \right\rangle = \mathrm{e}^{((n_1 + \ldots n_N)\alpha)} \left\langle \mathrm{e}^{(i(n_1\varphi_{x_1} + \ldots n_N\varphi_{x_N}))} \right\rangle$$

This implies that if $\sum_{n=1}^{N} n_i \neq 0, \text{ then } \left\langle \mathrm{e}^{(i(n_1\varphi_{x_1} + \cdots + n_N\varphi_{x_N}))} \right\rangle = 0$. In arXiv 1903.01918, we show that local tensor selection rules imply these identities.

The tensor formulation

At each link, we use the Fourier expansion

$$e^{\beta \cos(\varphi_{x+\hat{i}}-\varphi_x)} = \sum_{n_{x,i}=-\infty}^{+\infty} e^{in_{x,i}(\varphi_{x+\hat{i}}-\varphi_x)} I_{n_{x,i}}(\beta)$$

where the I_n are the modified Bessel functions of the first kind. After inegrating over the φ:

$$Z = I_0^V(\beta)\mathrm{Tr}\prod_x T^x_{(n_{x-\hat{1},1},n_{x,1},\dots,n_{x,D})}.$$

The local tensor T^x has $2D$ indices. The explicit form is

$$T^x_{(n_{x-\hat{1},1},n_{x,1},\dots,n_{x-\hat{D},D},n_{x,D})} = \sqrt{t_{n_{x-\hat{1},1}}t_{n_{x,1}},\dots,t_{n_{x-\hat{D},D}}t_{n_{x,D}}} \times \delta_{n_{x,out},n_{x,in}}$$

with $t_n \equiv I_n(\beta)/I_0(\beta)$ and

$$n_{x,in} = \sum_i n_{x-\hat{i},i} \text{ and } n_{x,out} = \sum_i n_{x,i}$$

Current conservation from $\delta_{n_{x,out},n_{x,in}}$

If we interpret the tensor indices $n_{x,i}$ with $i < D$ as spatial current densities and $n_{x,D}$ as a charge density, the Kronecker delta $\delta_{n_{x,out},n_{x,in}}$ in the tensor is a discrete version of Noether current conservation

$$\sum_i (n_{x,i} - n_{x-\hat{i},i}) = 0,$$

If we enclose a site x in a small D-dimensional cube, the sum of indices corresponding to positive directions ($n_{x,out}$) is the same as the sum of indices corresponding to negative directions ($n_{x,in}$).

We can “assemble" such elementary objects by tracing over indices corresponding to their interface and construct an arbitrary domain. Each tracing automatically cancels an in index with an out index and consequently, at the boundary of the domain, the sum of the in indices remains the same as the sum of the out indices.

Boundary conditions

- Periodic boundary conditions (PBC) allow us to keep a discrete translational invariance. As a consequence the tensors themselves are translation invariant and assembled in the same way at every site, link etc.
- Open boundary conditions (OBC) can be implemented by introducing new tensors that can be placed at the boundary. The only difference is that there are missing links at sites or missing plaquettes a links (zero index on “missing" links").

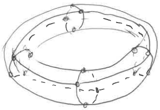

PBC

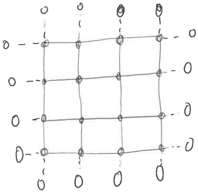

OBC

Explanation of the selection rule (YM 1903.01918)

$$\text{If } \sum_{n=1}^{N} n_i \neq 0, \quad \text{then } \langle e^{(i(n_1\varphi_{x_1}+\cdots+n_N\varphi_{x_N}))}\rangle = 0.$$

The insertion of various $e^{in_Q\varphi_x}$ is required in order to calculate the averages function $\langle e^{(i(n_1\varphi_{x_1}+\cdots+n_N\varphi_{x_N}))}\rangle$ This can be done by inserting an “impure" tensor which differs from the “pure" tensor by the Kronecker symbol replacement $\delta_{n_{x,out},n_{x,in}} \to \delta_{n_{x,out},n_{x,in}+n_Q}$.

In absence of insertions of $e^{in_Q\varphi_x}$, the Kronecker delta at the sites leads to a global conservation (sum in = sum out).

We can now repeat this procedure with insertions of $e^{in_Q\varphi_x}$. Each insertion adds n_Q, which can be positive or negative, to the sum of the out indices. We can apply this bookkeeping on an existing tensor configuration until we have gathered all the insertions and we reach the boundary of the system.

For PBC, this means that all the in and out indices get traced in pairs at the boundary. This is only possible if the sum of the inserted charges is zero which is the content of Eq. (22). For OBC, all the boundary indices are zero and the same conclusion apply.

In summary we have shown that the selection rule is a consequence of the Kronecker delta appearing in the tensor and is independent of the particular values taken by the tensors. So if we set some of the tensor elements to zero as we do in a truncation, this does not affect the selection rule.

TRG Formulation of 3D Z_2 Gauge Theory

$$Z = \sum_{\{\sigma\}} \exp\left(\beta \sum_P \sigma_{12}\sigma_{23}\sigma_{34}\sigma_{41}\right),$$

For each plaquette the weight is

$$\sum_{n=0,1} (\tanh(\beta)\sigma_{12}\sigma_{23}\sigma_{34}\sigma_{41})^n.$$

Regrouping the factors with a given σ_l and summing over ± 1 we obtain a tensor attached to this link

$$A^{(l)}_{n_1 n_2 n_3 n_4} = \delta\left(\mathrm{mod}[n_1 + n_2 + n_3 + n_4, 2]\right).$$

A and B tensors

The four links attached to a given plaquette p must carry the same index 0 or 1. For this purpose we introduce a new tensor

$$
\begin{aligned}
B^{(p)}_{m_1 m_2 m_3 m_4} &= \tanh(\beta)^{m_1}\delta(m_1, m_2, m_3, m_4) \\
&= \tanh(\beta)^{m_1}\begin{cases} 1, & \text{all } m_i \text{ are the same} \\ 0, & \text{otherwise.} \end{cases}
\end{aligned}
$$

The partition function can now be written as

$$
Z = (2\cosh\beta)^{3V}\mathrm{Tr}\prod_l A^{(l)}_{n_1 n_2 n_3 n_4}\prod_p B^{(p)}_{m_1 m_2 m_3 m_4},
$$

The procedure is manifestly gauge invariant. For $U(1)$ gauge theories, replace $tanh(\beta)^m$ by $I_m(\beta)$.

A and B tensors graphically

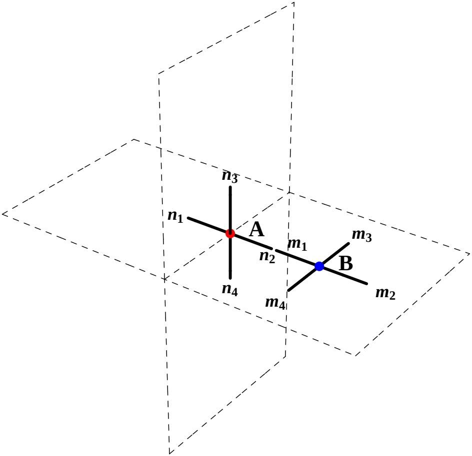

$\langle e^{iA_{x,i}} \rangle = 0$ for pure gauge $U(1)$ (arXiv 1903.01918)

- We assign “in” and “out" qualities to the legs of the A-tensors.
- For a given pair of directions i and j, there are 8 types of legs for the A-tensors that we label $[(x,i),\pm\hat{j}]$, $[(x-\hat{i},i),\pm\hat{j}]$, $[(x,j),\pm\hat{i}]$, and $[(x-\hat{j},j),\pm\hat{i}]$.
- The $[(x,i),\hat{j}]$ with $i<j$ are given an out assignment.
- There are three operations that swap in and out: changing (x,i) into $(x-\hat{i},i)$, changing $\hat{j}$ into $-\hat{j}$ and interchanging i and j.
- A detailed inspection shows that this assignment gives consistent in-out assignments at the B tensors and that the assignment is compatible with our sign partition.
- The Kronecker delta appearing at any link is independently enforced by the Kronecker deltas on the $2D-1$ other links attached to x and if we insert $e^{iA_{x,i}}$ the conditions become incompatible which implies $\langle e^{iA_{x,i}} \rangle = 0$.

Pure gauge D= 2 and 3

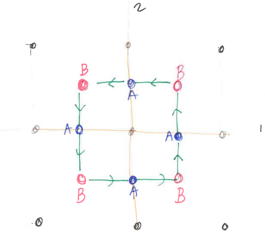

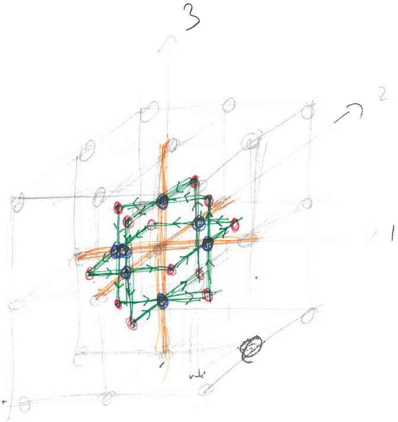

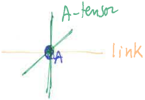

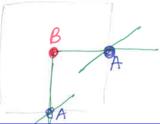

TRG approach of the transfer matrix

The partition function can be expressed in terms of a transfer matrix:

$$Z = \mathrm{Tr}\, \mathbb{T}^{L_t} \ .$$

The matrix elements of $\mathbb{T}$ can be expressed as a product of tensors associated with the sites of a time slice (fixed t) and traced over the space indices (PhysRevA.90.063603)

$$\mathbb{T}_{(n_1,n_2,\dots n_{L_x})(n'_1,n'_2\dots n'_{L_x})} = \sum_{\tilde{n}_1\tilde{n}_2\dots\tilde{n}_{L_x}} T^{(1,t)}_{\tilde{n}_{L_x}\tilde{n}_1 n_1 n'_1} T^{(2,t)}_{\tilde{n}_1\tilde{n}_2 n_2 n'_2\dots} \dots T^{(L_x,t)}_{\tilde{n}_{L_{x-1}}\tilde{n}_{L_x} n_{L_x} n'_{L_x}}$$

with (for the $O(2)$ model with chemical potential)

$$T^{(x,t)}_{\tilde{n}_{x-1}\tilde{n}_x n_x n'_x} = \sqrt{I_{n_x}(\beta_\tau) I_{n'_x}(\beta_\tau) I_{\tilde{n}_{x-1}}(\beta_s) I_{\tilde{n}_x}(\beta_s) \mathrm{e}^{(\mu(n_x+n'_x))}}\, \delta_{\tilde{n}_{x-1}+n_x,\tilde{n}_x+n'_x}$$

The Kronecker delta function reflects the existence of a conserved current, a good quantum number (“particle number"). In the limit $\beta_\tau \to \infty$ we get the Hamiltonian ($\mathbb{T} \simeq 1 - (1/\beta_\tau)\hat{H}$).

Transfer matrix with TRG

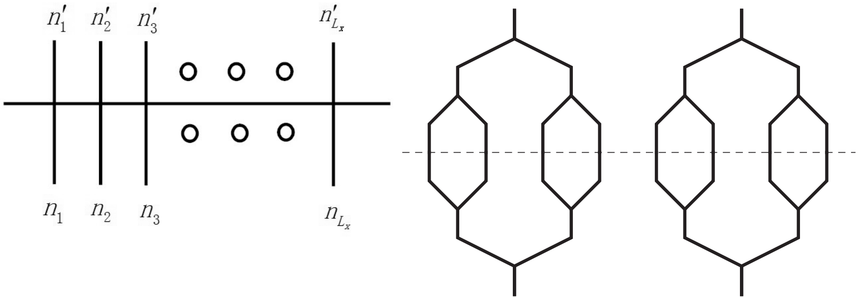

Figure: Graphical representation of the transfer matrix (left) and its successive coarse graining (right). See PRD 88 056005 and PRA 90, 063603 for explicit formulas.

Algebraic aspects (in one dimension)

In the Hamiltonian formalism, we introduce the angular momentum eigenstates which are also energy eigenstates

$$\hat{L}|n\rangle = n|n\rangle, \hat{H}|n\rangle = \frac{n^2}{2}|n\rangle$$

We assume that n can take any integer value from $-\infty$ to $+\infty$. As $\hat{H} = (1/2)\hat{L}^2$, it is obvious that $[\hat{L}, \hat{H}] = 0$.

The insertion of $\mathrm{e}^{i\varphi_x}$ in the path integral, translates into as operator $\widehat{\mathrm{e}^{i\varphi}}$ which raises the charge $\widehat{\mathrm{e}^{i\varphi}}|n\rangle = |n+1\rangle$, while its Hermitean conjugate lowers it $(\widehat{\mathrm{e}^{i\varphi}})^\dagger|n\rangle = |n-1\rangle$.

This implies the commutation relations

$$[L, \widehat{\mathrm{e}^{i\varphi}}] = \widehat{\mathrm{e}^{i\varphi}},\ [L, \widehat{\mathrm{e}^{i\varphi}}^\dagger] = -\widehat{\mathrm{e}^{i\varphi}}^\dagger, [\widehat{\mathrm{e}^{i\varphi}}, \widehat{\mathrm{e}^{i\varphi}}^\dagger] = 0.$$

Truncation effects on algebra

By truncation we mean that there exists some n_{max} for which

$$\widehat{e^{i\varphi}}|n_{max}\rangle = 0, \text{and } (\widehat{e^{i\varphi}})^\dagger|-n_{max}\rangle = 0.$$

The only changes the commutation relations are

$$\begin{aligned} \langle n_{max}|[\widehat{e^{i\varphi}}, \widehat{e^{i\varphi}}^\dagger]|n_{max}\rangle &= 1, \\ \langle -n_{max}|[\widehat{e^{i\varphi}}, \widehat{e^{i\varphi}}^\dagger]|-n_{max}\rangle &= -1, \end{aligned} \tag{1}$$

instead of 0. The truncation only affects matrix elements involving the $\widehat{e^{i\varphi}}$ operators but does not contradict that: If $\sum_{n=1}^{N} n_i \neq 0$, then $\langle 0|(\widehat{e^{i\varphi}})^{n_1} \dots (\widehat{e^{i\varphi}})^{n_N}|0\rangle = 0$ (with $(\widehat{e^{i\varphi}})^{-n} \equiv (\widehat{e^{i\varphi}}^\dagger)^n$ for $n > 0$))
Note: similar questions appear in quantum links formulations (see R. Brower, The QCD Abacus, hep-lat/9711027)

Rényi entanglement entropy

The n -th order Rényi entanglement entropy is defined as:

$$S_n(A) \equiv \frac{1}{1-n} \ln(\mathrm{Tr}\,((\hat{\rho}_A)^n)) \ .$$

$\lim_{n\to 1^+} S_n$=von Neumann entanglement entropy.

The approximately linear behavior in $\ln(N_s)$ is consistent with the logarithmic scaling which predicts

$$S_n(N_s) = K + \frac{c(n+1)}{6n} \ln(N_s)$$

for periodic boundary conditions and half the slope ($\frac{c(n+1)}{12n}$) for open boundary conditions. c is the central charge. The constant K is non-universal and different in the four situations considered (n=1, 2 with PBC and OBC).

References for the logarithmic formula

- C. Holzhey, F. Larsen and F. Wilczek, Nucl. Phys. B 424, 443, (1994)
- G. Vidal, J.I. Latorre, E. Rico, and A. Kitaev, Phys. Rev. Lett. 90 , 227902-1 (2003)
- V.E. Korepin, Physical Review Letters, vol 92, issue 9, electronic identifier 096402, 05 March 2004, arXiv:cond-mat/0311056
- B.-Q.Jin, V.E.Korepin, Journal of Statistical Physics , vol 116, Nos. 1-4, page 79, 2004
- P. Calabrese and J. Cardy, Journal of Statistical Mechaics: Theory and Experiment 2004, P06002 (2004).

Entanglement entropy S_E (PRE 93, 012138 (2016))

We consider the subdivision of AB into A and B (two halves in our calculation) as a subdivision of the spatial indices.

$$\hat{\rho}_A \equiv \mathrm{Tr}_B \hat{\rho}_{AB}; \quad S_{EvonNeumann} = -\sum_i \rho_{A_i} \ln(\rho_{A_i}).$$

We use blocking methods until A and B are each reduced to a single site.

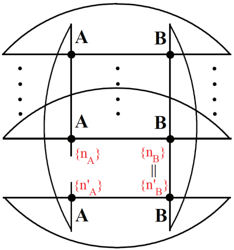

Figure: The horizontal lines represent the traces on the space indices. There are L_t of them, the missing ones being represented by dots. The two vertical lines represent the traces over the blocked time indices in A and B.

Bose-Hubbard & $O(2)$ Phase Diagram PRA 96 023603 (2017), PRD 96 034514 (2017)

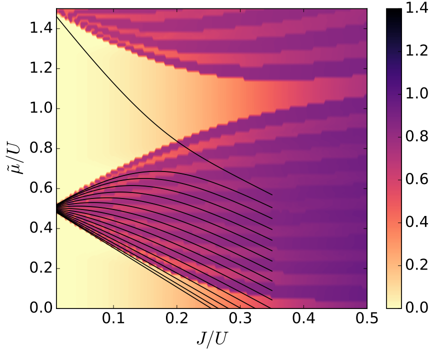

- $N_s = 16$ lattice
- Color is S_2 for time-continuum $O(2)$.
- The light lobes are Mott insulator regions
- The stripes are jumps in particle number
- In black are the particle number boundaries for BH

Numerical results

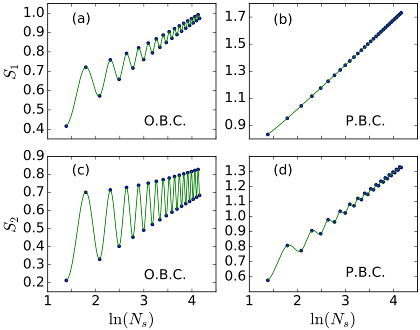

Figure: The first order and second order Rényi entropy scaling with system size for $\beta_s\beta_\tau = 0.01$, $\mu\beta_\tau = 0.5$ in the time continuum limit calculated using DMRG. (a), (b) The first order Rényi entropy with OBC and PBC respectively. (c), (d) The second order Rényi entropy with OBC and PBC respectively. Oscillations are understood in CFT (Cardy and Calabrese).

Left

- Two identical copies are made
- A beamsplitter operation is applied across the copies
- The resulting parities at each site in a copy give the quantum purity ($\exp(-S_2) = Tr\rho_A^2 =< (-1)^{\sum_{x\in A} n_x(1 copy)} >$)

Right (preparation)

- A Mott state is prepared.
- Harmonic confinement.
- J/U is tuned.
- Confinement is removed.

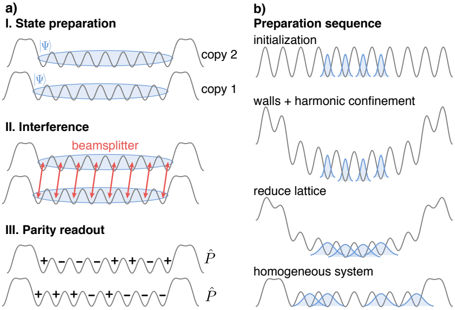

Quantum Joule expansions (arXiv:1903.01414)

Quantum Joule Expansion of One-dimensional Systems

Jin Zhang[1], Y. Meurice[2], and S.-W. Tsai[1]
[1]*Department of Physics and Astronomy, University of California, Riverside, CA 92521, USA and*
[2]*Department of Physics and Astronomy, University of Iowa, Iowa City, IA 52242, USA*
(Dated: March 5, 2019)

We investigate the Joule expansion of nonintegrable quantum systems that contain bosons or fermions in one-dimensional lattices. A barrier initially confines the particles to be in half of the system in a thermal state described by the canonical ensemble. At long times after the barrier is removed, few-body observables can be approximated by a thermal expectation of another canonical ensemble with an effective temperature. The weights for the diagonal ensemble and the canonical ensemble match well for high initial temperatures that correspond to negative effective final temperatures after the expansion. The negative effective temperatures for finite systems go to positive inverse temperatures in the thermodynamic limit for bosons, but is a true thermodynamic effect for fermions. We compare the thermal entanglement entropy and density distribution in momentum space for the canonical ensemble, diagonal ensemble and instantaneous long-time states calculated by exact diagonalization. We propose the Joule expansion as a way to dynamically create negative temperature states for fermion systems.

I. INTRODUCTION

With the remarkable advances in efficient computing algorithms and cold atom experiments, nonequilibrium dynamics has been extensively studied both theoretically and experimentally in recent years. Quantum thermalization is one of the most important topics in this area. In 1929, the classical theory of statistical mechanics was reformulated quantum-mechanically by von Neumann [1], which opens the door to the study of quantum thermalization through the unitary dynamics of quantum sys-

states [18, 23].

A celebrated experiment in the context of classical statistical mechanics is the Joule expansion. The Joule expansion (free expansion) of an ideal gas from an initial volume V to a final volume $2V$ does not change the temperature of the gas and the increase in entropy is $nR\ln 2$. For interacting gases, the temperature decreases for attractive interactions, such as for the van der Waals gas, and increases for repulsive interactions. But what happens for quantum systems? The Joule expansion of an isolated perfect quantum gas is discussed in [24], where

Temperature before and after expansion (arXiv:1903.01414)

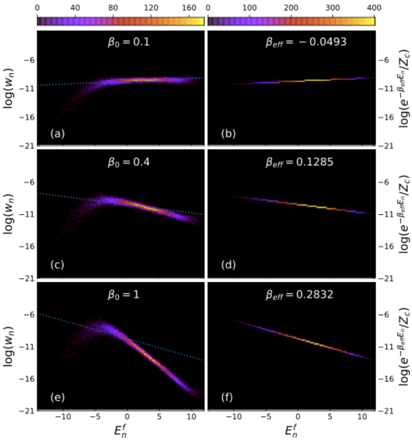

FIG. 1. (Color online) Two-dimensional histograms for the weights of eigenstates in the DE, W_n, (a,c,e) and those in the corresponding CE $e^{-\beta_{eff}E_n}/Z(\beta_{eff})$ (b,d,f). Results are for spinless fermions with 20 sites, 5 particles and $J_2 = V_2 = 1$.

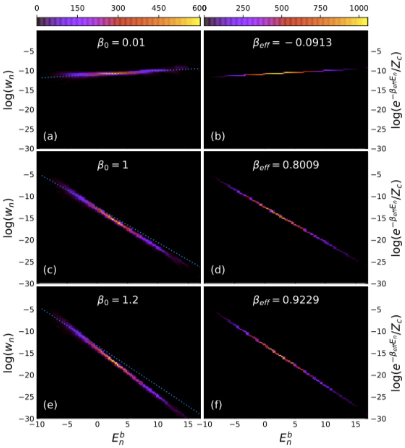

FIG. 2. (Color online) Same as Fig. 1, but for bosons with 20 sites, 5 particles and $U = 3$.

Momentum distribution functions (arXiv:1903.01414)

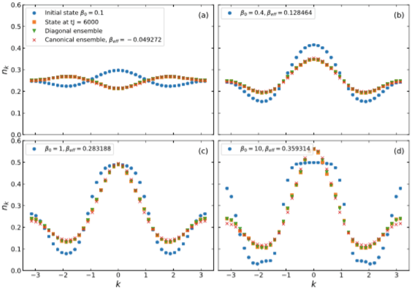

FIG. 13. (Color online) MDFs of the initial state, the time-evolved state at $tJ = 6000$, the DE and the corresponding CE as a function of momentum $k \in (-\pi, \pi)$. The results are for spinless fermions, with different initial inverse temperatures $\beta_0 = 0.1$ (a), $\beta_0 = 0.4$ (b), $\beta_0 = 1$ (c) and $\beta_0 = 10$ (d).

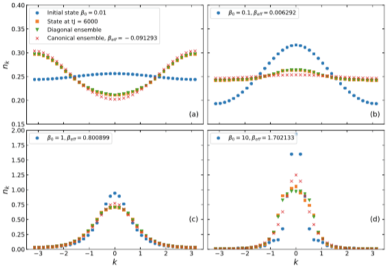

FIG. 14. The same with Fig. 13 but for bosons. The initial inverse temperatures are $\beta_0 = 0.01$ (a), $\beta_0 = 0.1$ (b), $\beta_0 = 1$ (c) and $\beta_0 = 10$ (d).

The compact Abelian Higgs model

This is a gauged $O(2)$ model with gauge fields on the links $A_{x,\hat{i}}$.

$$\int \mathcal{D}\Phi = \prod_x \int_{-\pi}^{\pi} \frac{d\varphi_x}{2\pi} \prod_{x,i} \int_{-\pi}^{\pi} \frac{dA_{x,i}}{2\pi}.$$

$$S = -\beta \sum_{x,i} \cos(\varphi_{x+\hat{i}} - \varphi_x + A_{x,i}) - \beta_p \sum_{x,i<j} \cos(A_{x,i} + A_{x+\hat{i},j} - A_{x+\hat{i}+\hat{j},i} - A_{x,j}).$$

The symmetry of the $O(2)$ model becomes local

$$\varphi'_x = \varphi_x + \alpha_x \text{ and } A'_{x,i} = A_{x,i} - (\alpha_{x+\hat{i}} - \alpha_x),$$

Truncations do not break these symmetries (Y. M. arXiv 1901.01918).
For Hamiltonian and optical lattice implementations see: Phys. Rev. D 92, 076003 (2015), Phys. Rev. Lett. 121, 223201 (2018)

Optical lattice implementation of the compact Abelian Higgs Model with a physical ladder (see Judah Unmuth-Yockey 's talk and PRL 121, 223201)

After taking the time continuum limit:

$$\bar{H} = \frac{\tilde{U}_g}{2}\sum_i \left(\bar{L}^z_{(i)}\right)^2 + \frac{\tilde{Y}}{2}\sum_i(\bar{L}^z_{(i)} - \bar{L}^z_{(i+1)})^2 - \tilde{X}\sum_i \bar{L}^x_{(i)}$$

5 states ladder with 9 rungs

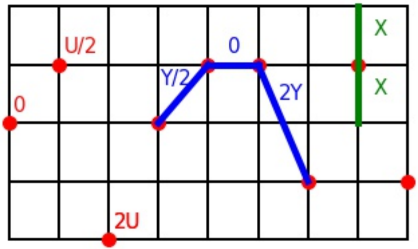

Gauge-invariant tensor form: $Z = Tr[\prod T]$

(see PRD.88.056005 and PRD.92.076003)

$$Z = \propto \mathrm{Tr}\left[\prod_{h,v,\Box} A^{(s)}_{m_{up}m_{down}} A^{(\tau)}_{m_{right}m_{left}} B^{(\Box)}_{m_1 m_2 m_3 m_4}\right].$$

The traces are performed by contracting the indices as shown

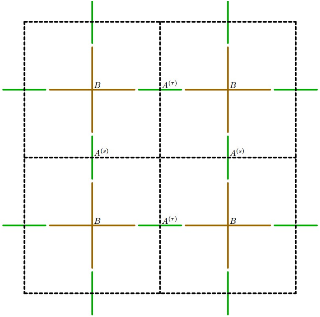

Polyakov loop: definition

Polyakov loop, a Wilson line wrapping around the Euclidean time direction: $\langle P_i \rangle = \langle \prod_j U_{(i,j),\tau} \rangle$ =exp($-F(\text{single charge})/kT$); the order parameter for deconfinement.

With periodic boundary condition, the insertion of the Polyakov loop (red) forces the presence of a scalar current (green) in the opposite direction (left) or another Polyakov loop (right).

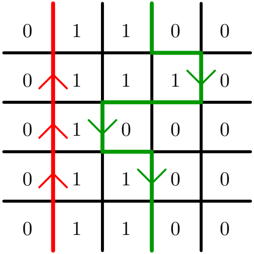

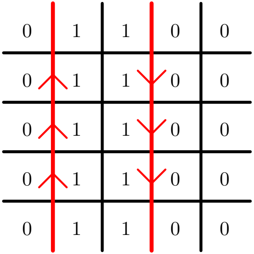

In the Hamiltonian formulation, we add $-\frac{\tilde{Y}}{2}(2(\bar{L}^z_{i^\star} - \bar{L}^z_{(i^\star+1)}) - 1)$ to H.

Universal functions (FSS): the Polyakov loop

arXiv:1803.11166 (Phys. Rev. Lett. 121, 223201) and
arXiv:1807.09186 (Phys. Rev. D 98, 094511)

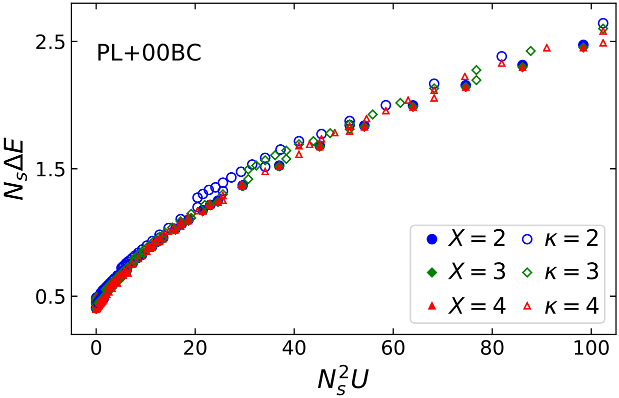

Figure: Data collapse of $N_s \Delta E$ defined from the insertion of the Polyakov loop, as a function of $N_s^2 U$, or $(N_s g)^2$ (collapse of 24 datasets). Numerical work by Judah Unmuth-Yockey and Jin Zhang.

A first quantum simulator for the abelian Higgs model?

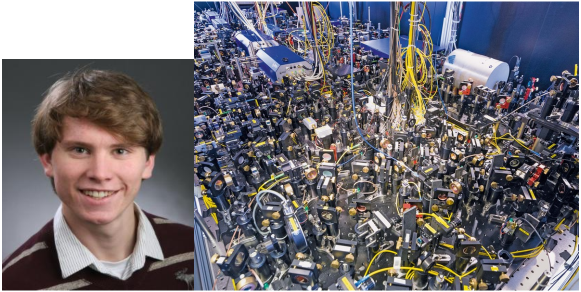

Figure: Left: Johannes Zeiher, a recent graduate from Immanuel Bloch's group can design ladder shaped optical lattices with nearest neighbor interactions. Right: an optical lattice experiment of Bloch's group.

Concrete Proposal (PRL 121, 223201)

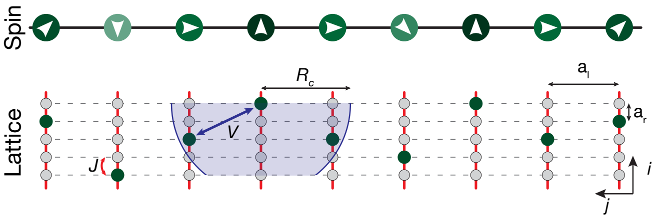

Figure: Multi-leg ladder implementation for spin-2. The upper part shows the possible m_z-projections. Below, we show the corresponding realization in a ladder within an optical lattice. The atoms (green disks) are allowed to hop within a rung with a strength J, while no hopping is allowed along the legs. The lattice constants along rung and legs are a_r and a_l respectively. Coupling between atoms in different rungs is implemented via an isotropic Rydberg-dressed interaction V with a cutoff distance R_c (marked by blue shading).

Quantum Ising model (2 legs): Looking at the vacuum wavefunction: σ^z meas. (N qubits!, at LMU or MPQ?)

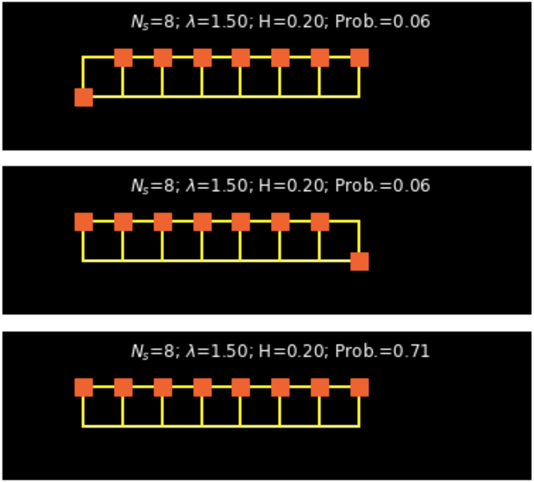

The quantum Ising model

It is possible to take the time continuum limit for the classical model in 1+1 dimensions and keep the spatial lattice. This result into the quantum hamiltonian in one space dimension.

$$\hat{H} = -J \sum_i \hat{\sigma}_i^z \hat{\sigma}_{i+1}^z - h_T \sum_i \hat{\sigma}_i^x - h_L \sum_i \hat{\sigma}_i^z$$

Often the energies are expressed in units of the transverse magnetic field h_T. $\lambda \equiv J/h_t$ with $\lambda_c = 1$. In the ladder realization, h_T is proportional to the inverse tunneling time along the rungs. The zero temperature magnetic susceptibility is

$$\chi^{quant.} = \frac{1}{L} \sum_{<i,j>} < (\sigma_i - < \sigma_i >)(\sigma_j - < \sigma_j >) > \propto \xi^{1-\eta} \propto |\lambda - 1|^{-\nu(1-\eta)}$$

where $< ... >$ are short notations for $\langle \Omega | ... | \Omega \rangle$ with $|\Omega\rangle$ the lowest energy state of $\hat{H}$.

Data collapse for the quantum magnetic susceptibility: $\chi^{quant.\prime} = \chi^{quant.} L^{-(1-\eta)}$ versus $\lambda' = L^{1/\nu}(\lambda - 1)$

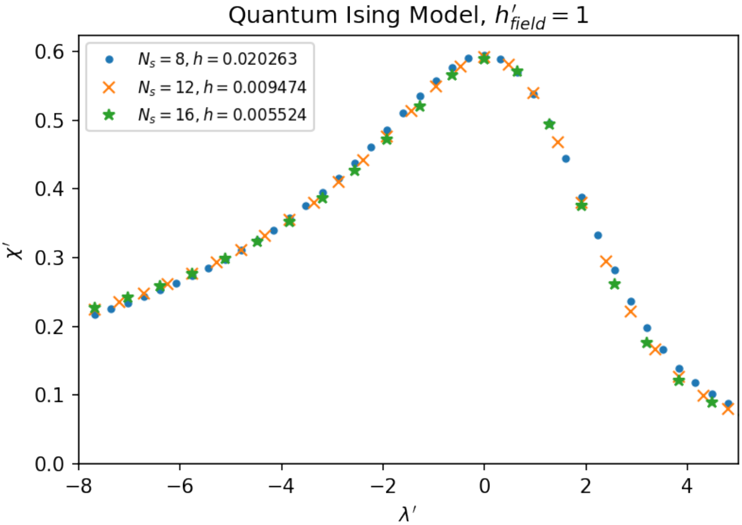

The Schwinger model (in progress with N. Butt, S. Catterall and J. Unmuth-Yockey)

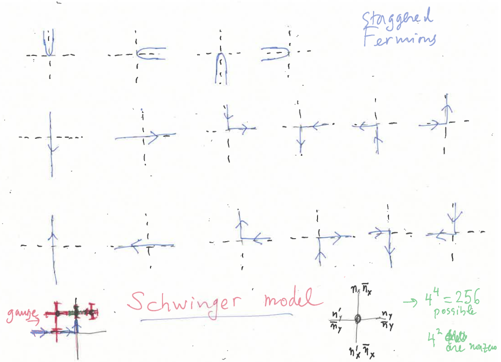

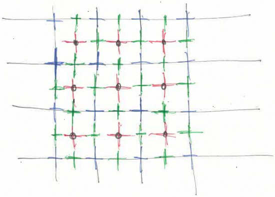

No sign issue (to be confirmed)

Schwinger model with trapped ions

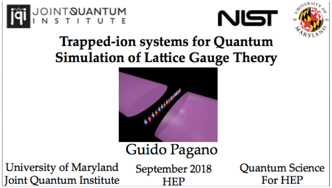

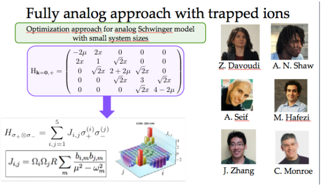

Figure: From Guido Pagano talk at Fermilab.

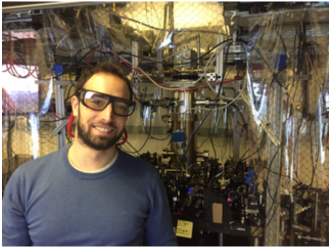


Google AI
Quantum
Automatic calibration of arrays of superconducting qubits and couplers
Kevin Satzinger (ksatz@google.com)
APS March Meeting A42.5
March 4, 2019


Measuring and quantifying classical crosstalk in multi-qubit superconducting circuits
Petar Jurcevic, Abhinav Kandala, Antonio Corcoles,
Jerry M. Chow, Jay Gambetta
IBM Q

Time evolution with QC: IBM and Rigetti

PHYSICAL REVIEW A **98**, 032331 (2018)

Quantum-classical computation of Schwinger model dynamics using quantum computers

N. Klco,[1,*] E. F. Dumitrescu,[2] A. J. McCaskey,[3] T. D. Morris,[4] R. C. Pooser,[2] M. Sanz,[5] E. Solano,[5,6] P. Lougovski,[2,†] and M. J. Savage[1,‡]

[1]*Institute for Nuclear Theory, University of Washington, Seattle, Washington 98195-1550, USA*
[2]*Computational Sciences and Engineering Division, Oak Ridge National Laboratory, Oak Ridge, Tennessee 37831, USA*
[3]*Computer Science and Mathematics Division, Oak Ridge National Laboratory, Oak Ridge, Tennessee 37831, USA*
[4]*Physics Division, Oak Ridge National Laboratory, Oak Ridge, Tennessee 37831, USA*
[5]*Department of Physical Chemistry, University of the Basque Country UPV/EHU, Apartado 644, E-48080 Bilbao, Spain*
[6]*IKERBASQUE, Basque Foundation for Science, Maria Diaz de Haro 3, E-48013 Bilbao, Spain*

(Received 22 March 2018; published 28 September 2018)

We present a quantum-classical algorithm to study the dynamics of the two-spatial-site Schwinger model on IBM's quantum computers. Using rotational symmetries, total charge, and parity, the number of qubits needed to perform computation is reduced by a factor of $\sim$5, removing exponentially large unphysical sectors from the Hilbert space. Our work opens an avenue for exploration of other lattice quantum field theories, such as quantum chromodynamics, where classical computation is used to find symmetry sectors in which the quantum computer evaluates the dynamics of quantum fluctuations.

PHYSICAL REVIEW LETTERS **121**, 170501 (2018)

Simulation of Nonequilibrium Dynamics on a Quantum Computer

Henry Lamm[*] and Scott Lawrence[†]
Department of Physics, University of Maryland, College Park, Maryland 20742, USA

(Received 21 June 2018; revised manuscript received 6 September 2018; published 22 October 2018)

We present a hybrid quantum-classical algorithm for the time evolution of out-of-equilibrium thermal states. The method depends on classically computing a sparse approximation to the density matrix and, then, time-evolving each matrix element via the quantum computer. For this exploratory study, we investigate a time-dependent Ising model with five spins on the Rigetti Forest quantum virtual machine and a one spin system on the Rigetti 8Q-Agave quantum processor.

From tensors to circuits

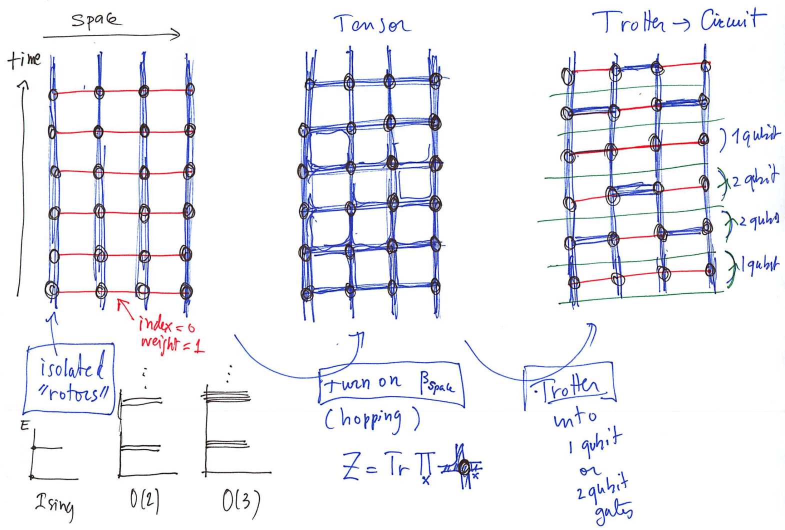

Quantum circuit for the quantum Ising model

Quantum circuit with 3 Trotter steps (arXiv:1901.05944 E. Gustafson, YM and J. Unmuth-Yockey, PRD 99 094503)

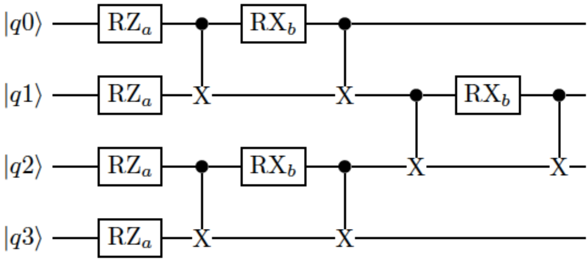

Figure 1: Circuit for 4 qubits with open boundary conditions

Trotter Fidelity

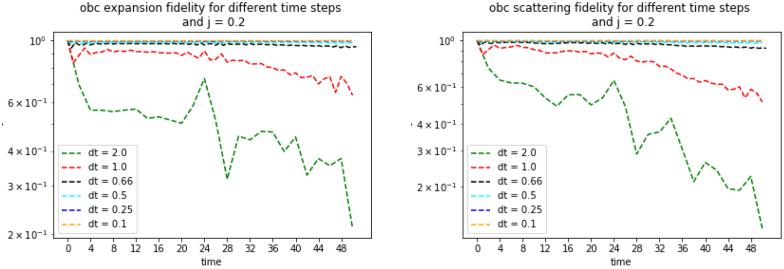

Figure: fidelity of Trotter operator at multiple different Trotter steps for (left to right) expansion and scattering with open boundary conditions (E. Gustafson, YM and J. Unmuth-Yockey arXiv:1901.05944, PRD 99 094503)

Systematic and statistical errors

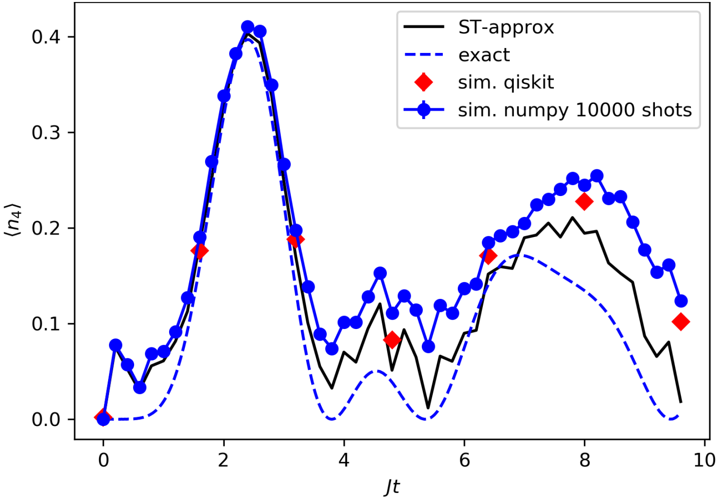

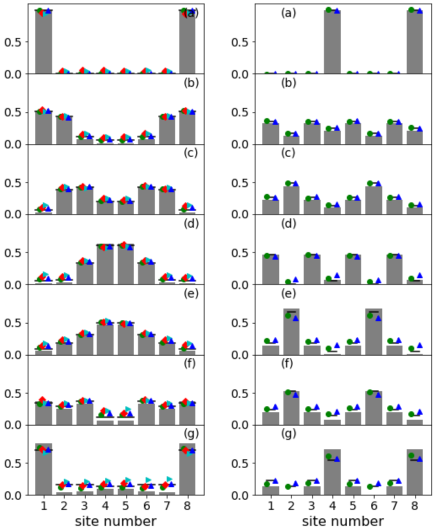

Figure: Evolution of two-particle initial states with OBC (Left) and PBC (Right). Simulations with QISKIT and numpy for current trapped ions or near future superconducting qubits (arXiv:1901.05944, PRD 99 094503).

Conclusions

- QC/QIS in HEP and NP: we need big goals with many intermediate steps
- Tensor Field Theory is a generic tool to discretize path integral formulations of lattice model with compact variables
- TRG: exact blocking, a friendly competitor to QC
- Truncations respect symmetries
- TRG: gauge-invariant approach for the quantum simulation of gauge models.
- Finite size scaling: small systems are interesting
- Real time scattering can be calculated with digital or analog methods (comparison is possible)
- Need for quantum simulations and computations facilities dedicated to theoretical physics
- Thanks!

Acknowledgements:

This research was supported in part by the Dept. of Energy under Award Numbers DOE grants DE-SC0010113, and DE-SC0019139